Could aerosol emissions be used for regional heat wave mitigation?

D. N. Bernstein[1,2]**, J. D. Neelin**[2]**, Q. B. Li**[2]**, and D. Chen**[2]

[1]Department of Soil and Water Sciences, Robert H. Smith Faculty of Agriculture, Food and Environment, The Hebrew University of Jerusalem, POB 12, Rehovot 76100, Israel
[2]Department of Atmospheric and Oceanic Sciences, University of California, Los Angeles, 405 Hilgard Ave., Los Angeles, CA 90095, USA

Abstract. Geoengineering applications by injection of sulfate aerosols into the stratosphere are under consideration as a measure of last resort to counter global warming. Here adaptation to a potential regional-scale application to offset the impacts of heat waves is critically examined. The effect of regional-scale sulfate aerosol emission over California in each of two days of the July 2006 heat wave using the Weather Research Forecast model with fully coupled chemistry (WRF-Chem) is used to quantify potential reductions in surface temperature as a function of emission rates in the lower stratosphere. Over the range considered, afternoon temperature reductions scale almost linearly with emissions. Local meteorological factors yield geographical differences in surface air temperature sensitivity. For emission rates of approximately 30 μg m^{-2} s^{-1} of sulfate aerosols (with standard WRF-Chem size distribution) over the region, temperature decreases of around 7°C result during the middle part of the day over the Central Valley, one of the hardest hit by the heat wave. Regions more ventilated with oceanic air such as Los Angeles have slightly smaller reductions. The length of the hottest part of the day is also reduced. Advection effects on the aerosol cloud must be more carefully forecast for smaller emission regions. Verification of the impacts could be done via measurements of differences in reflected and surface downward shortwave. Such regional geoengineering applications with specific near-term target effects but smaller cost and side effects could potentially provide a means of testing larger scale applications. However, design trade-offs differ from global applications and the size of the required emissions and the necessity of emission close to the target region raise substantial concerns. The evaluation of this regional scale application is thus consistent with global model evaluations emphasizing that mitigation via reduction of fossil fuels remains preferable to considering geoengineering with sulfate aerosols.

1 Introduction

Global surface temperatures are expected to rise over the coming century due to the ongoing emission of greenhouse gases, with attendant changes in frequency of extreme events such as heat waves (IPCC, 2007). Geoengineering solutions are under discussion as a potential means of offsetting this rise. A particular solution that has been proposed includes injecting sulfate aerosols into the stratosphere and cooling the earth's surface by reflecting incoming shortwave flux. Initially proposed by Budyko (1974), this has been controversial for obvious reasons. Because the effort to reduce greenhouse gas emissions is failing, however, the proposal has come into vogue again. Since serious consideration by Crutzen (2006), there have been a number of studies quantifying the effects of the global scale (Rasch et al., 2008; Robock et al., 2008; Brovkin et al., 2009; Jones et al., 2010; Kravitz et al., 2011; Niemeier et al., 2011; Volodin et al., 2011), and a number of studies raising substantial concerns regarding side effects (Matthews and Caldeira, 2007; Trenberth and Dai, 2007; Robock, 2008; Tilmes et al., 2008; Heckendorn et al., 2009; Kravitz et al., 2009; Robock et al., 2010). Crutzen (2006) estimated that the insertion of approximately 5 Tg per year of sulfur would be required to balance the impact of greenhouse gas warming in the case of a double-CO_2 emission scenario. Wigley (2006) suggested that an annual 5 Tg sulfur flux would be sufficient, alongside a reduction in emissions, while Pierce et al. (2010) and English et al. (2012) consider 10 Tg S yr^{-1}. The geoengineering injection of sulfate aerosols can be compared to those coming from a volcanic eruption. For example, Robock (2002), based on the eruption of Mount Pinatubo in June of 1991, estimated that about 20 Tg of SO_2 was released, which caused up to 2°C of cooling in surface temperatures with Northern Hemisphere con-

Correspondence to: J. David Neelin
(neelin@atmos.ucla.edu)

tinents in the summer of 1992. Rasch et al. (2008) pointed out that the impact of the aerosol emissions depends on the size of the inserted aerosols, and that smaller-sized aerosols scatter more efficiently.

The present study is motivated by the argument that it is useful for groups whose primary research focus lies elsewhere to contribute to evaluation of potential geoengineering proposals, especially where tools developed for other purposes can contribute at low cost to particular aspects of understanding the issues involved. While sharing deep reservations regarding the wisdom of geoengineering, we here use a setup of the the Weather Research Forecast model with fully coupled chemistry (WRF-Chem) (Grell et al., 2005) that has been used for air quality studies over California (Chen et al., 2012) to provide a model-based evaluation of one potential application of geoengineering. It is worth underlining that the technology to do such an experiment in the real world does not currently exist, but there is active research on such methods, including patent applications (Chan et al., 2010). Given this, it is important to have model-based studies to help to put into perspective what would be implied if such methods should become available.

In particular, this study examines whether aerosol emissions, specifically those which are being considered for global scale geoengineering, could be applied at the regional scale with the timing chosen to mitigate heat waves, or excessively hot weather events. If negative impacts of global warming create pressure for regional planners to enact geoengineering solutions, there are a number of factors that may bring regional-scale interventions to the forefront of the debate. Regional actions might involve less concerted effort and less international cooperation than a global scale application. Because global warming is tending to affect regions differently, regional geoengineering solutions could prove more feasible than their proposed global counterparts. Finally, smaller-scale solutions could potentially provide a means of testing the larger scale applications. However, the design considerations are not exactly the same; here we consider injection of sulfate aerosols to impact shortwave radiation on a time scale less than a day in the regional application. Global applications allow for longer evolution time which may include gas phase formation of sulfate aerosols and substantial impacts of microphysical considerations including deposition (Pierce et al., 2010; English et al., 2012). The aspect of the problem considered here emphasizes advection and regional-scale impacts, while using a standard source treatment from WRF-Chem. The aim is to provide a sense of the meteorological factors that would need to be taken into account in evaluating any such potential application.

We choose the heat wave of July 2006 in California as a case study. During this abnormal event, extremely hot surface temperatures were observed, resulting in a death toll estimated to exceed 140 (Ostro et al., 2009). The heat wave lasted for 17 days and peaked on July 23rd (Gershunov et al., 2009). Figure 1 shows surface air temperatures simu-

lated by the WRF model for July 22nd and July 23rd, as detailed in section 2. The simulated highest temperatures in California were in a narrow region in the Central Valley between the ventilated coastal area and mountain ridge (see the Supplementary Material for surface air temperatures and upper-level flow patterns from the North American Regional Reanalysis, (Mesinger et al., 2006)). The upper-level flow field is northerly over much of the domain at 200 mbar with speeds ranging from roughly 4 to 14 m/s over California. Heat waves may not evolve in exactly the same manner in future climate. However, the example of the recent heat wave serves to provide an upper-level flow field of reasonable magnitude and pattern, which is important to the advection of emitted aerosols, and a temperature simulation that yields high temperatures in a geographic pattern that is meteorologically reasonable.

The first point to address is whether advection rapidly carries the emitted aerosols away from the target region. Subsequent points of examination are quantifying the potential size of the reduction in surface solar radiation and reduction in surface air temperature (relative to the control simulation) for a given size of emission, and whether the meteorology of certain regions makes such experiments more or less effective.

2 Large-scale idealized experiment

2.1 Setup and advective effect

The Weather Research Forecast model with fully coupled chemistry (WRF-Chem) (Grell et al., 2005; Grell, 2008; Grell et al., 2011) is applied to simulate the impact of low stratospheric sulfate aerosols. The WRF-Chem is a non-hydrostatic mesoscale model that uses a terrain-following, hydrostatic-pressure vertical coordinate with the top of the model being a constant pressure surface. The horizontal structure of the model grid is the Arakawa-C grid. Here, the time integration scheme in the model uses a third-order Runge-Kutta scheme. The Yonsei University scheme (YSU, (Hong et al., 2004)) is used to parametrize the planetary boundary layer and Grell 3D ensemble scheme (Grell and Devenyi, 2002) for convective parameterization. The NOAA land-surface model (Chen and Dudhia, 2001) is used. The chemistry package includes dry deposition, aqueous phase chemistry coupled to some of the microphysics and aerosol schemes, biogenic emissions, anthropogenic emissions, chemical mechanisms, photolysis schemes, and aerosol schemes (Grell et al., 2005; Fast et al., 2006; Zaveri et al., 2008). The Model for Simulating Aerosol Interactions and Chemistry (MOSAIC) (Fast et al., 2006; Zaveri et al., 2008; Barnard et al., 2010) has been used for aerosol treatment. MOSAIC distributes aerosols according to their dry size into the discrete bins and calculates the mass and number for each bin. The standard option, four bins (0.039–0.156,
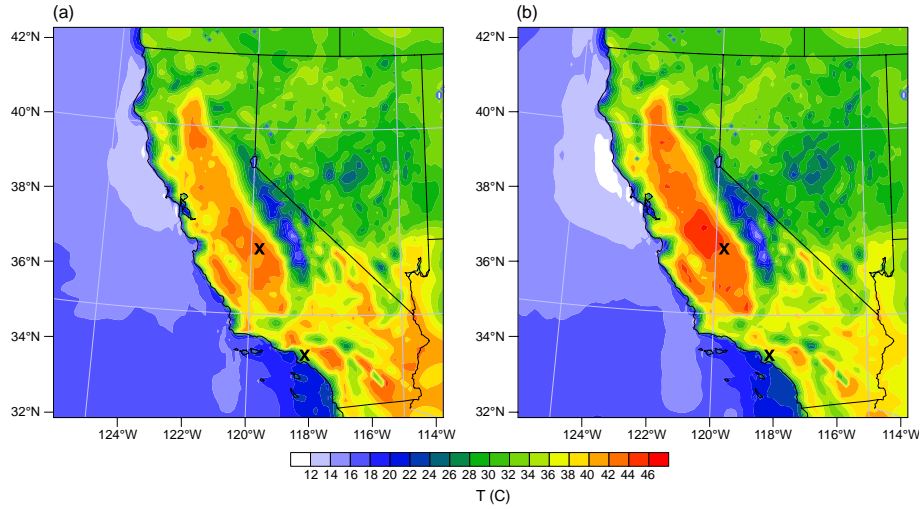
Fig. 1. Surface air temperature [°C] simulated by WRF for (a) 22 July 2006 and (b) 23 July 2006 over California and Nevada at 16:00 LT. Crosses show the sample locations in Los Angeles and the Central Valley used in Fig. 2.
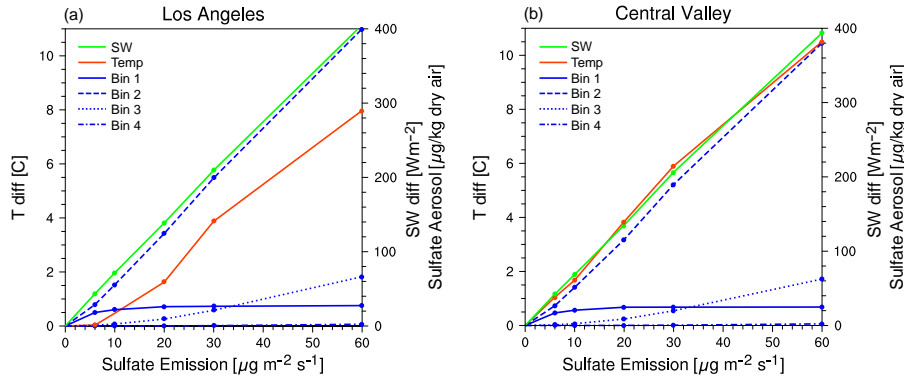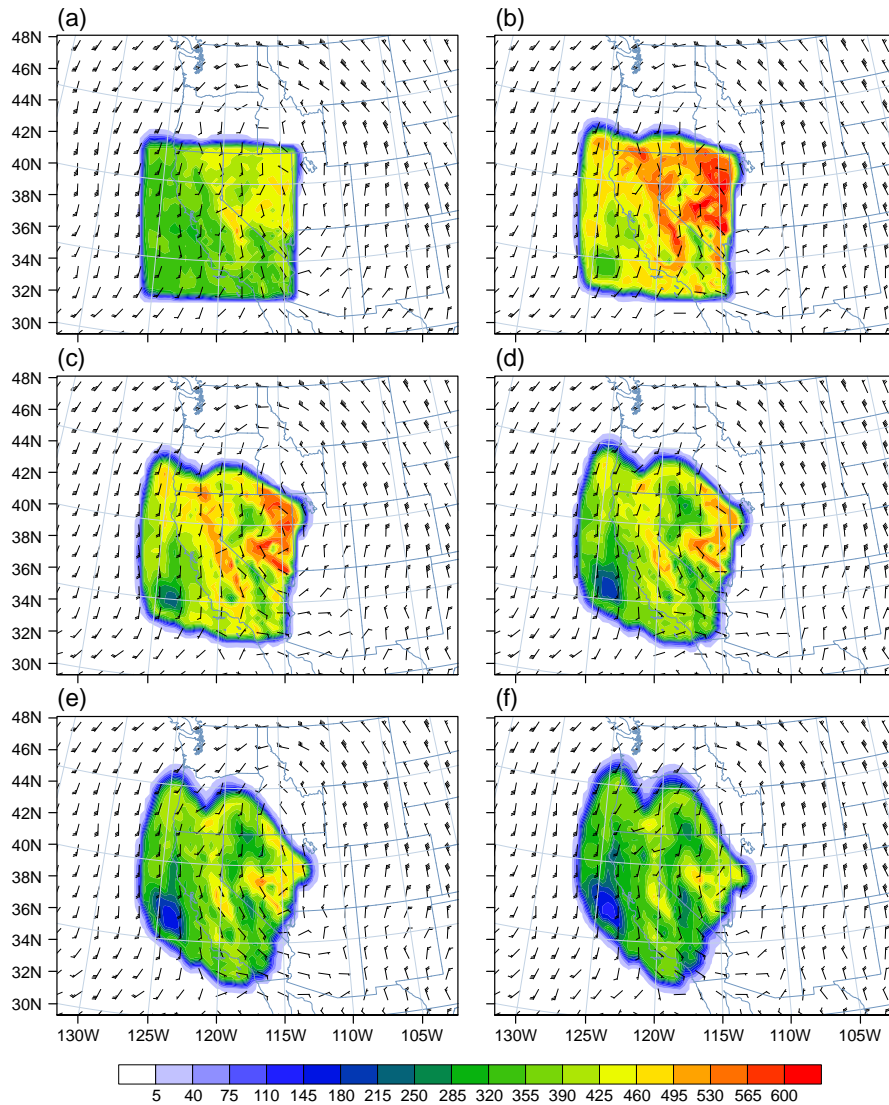

Fig. 2. Sulfate aerosol concentration in each bin [μg kg^{-1} of dry air] at the level of the injection with surface temperature [°C] and surface shortwave flux [W m^{-2}] differences as a function of the amplitude of aerosol emissions [μg m^{-2} s^{-1}] for the large-scale experiment at 13:00 LT in July 22nd for (a) a point in Los Angeles and (b) a point in the Central Valley (Fresno). See Fig. 1 for point locations. See section 2.1 for bin sizes, defined by dry particle diameter.

0.156–0.625, 0.625–2.5, 2.5–10.0 μm dry diameter) is used. The relevant aerosol species here is sulfate (SULF=SO$_4^{2-}$ + HSO$_4^-$). The size bins are defined by their lower and upper dry particle diameter, so water uptake or loss does not transfer particles between bins (Zaveri et al., 2008). Transfer of the mass between bins and particle growth is computed using the two-moment approach described by Tzivion et al. (1989). The aerosol optical properties, such as extinction, single-scattering albedo, and the asymmetry factor for scattering, are calculated as a function of wavelength and three-dimensional position. The refractive index, which is associated for each chemical constituent of the aerosol, is calculated by volume averaging for each size bin, and Mie theory is used to estimate the extinction efficiency and the scatter-

ing efficiency. For efficient computation of the extinction and the scattering efficiencies, WRF-Chem uses a methodology described by Ghan et al. (2001). After the aerosol radiative properties are calculated they are used in the shortwave radiative transfer model. A Dudhia shortwave radiative scheme is applied in our study to calculate the downward solar radiation flux, taking into account the diurnal variation of the solar zenith angle (Dudhia, 1989).

For this study we use version 3.1.1 of WRF-Chem, using the two-way nest option to increase resolution in an inner domain. The coarse model domain is configured covering the Western United States with a horizontal resolution of 36 km and 80 x 60 grid points, and the fine domain of California and Nevada with a horizontal resolution of 12 km and 97

Fig. 3. Bin 2 (0.156–0.625 μm) sulfate aerosol concentrations [μg kg^{-1} of dry air] and wind barbs (kts) at the level of the injection in July 22nd at hours (a) 8:00 LT, (b) 10:00 LT, (c) 12:00 LT, (d) 14:00 LT, (e) 16:00 LT, and (f) 18:00 LT.

x 97 grid points. The fine domain corresponds to the area shown in Fig. 1. The vertical structure of the model is 28 grid points with the top of the model at 50hPa. The initial and lateral boundary conditions for meteorological variables are obtained from the National Centers for Environmental Prediction Eta/North American Mesoscale model data set with 40 km spatial resolution at three-hour intervals (available from the Research Data Archive dataset number ds609.2 maintained at the National Center for Atmospheric Research http://dss.ucar.edu). Sea surface temperatures are specified from the same data set. The WRF-Chem emissions for all anthropogenic chemical species is based on the EPA 2005 National Emission Inventory (NEI 05). This setup follows the same model configuration as is validated by Chen et al.

(2012) during a field campaign in May 2010 in California. A similar configuration of WRF over California is used in several studies and evaluated against observations for various events (Bao et al., 2008; Lu et al., 2012). Chapman et al. (2009) used WRF-Chem with the MOSAIC aerosol scheme to study the radiative impact of elevated point sources, which showed good agreement with observed data. For consistency with these prior studies, we keep the emissions specification for sulfate aerosol exactly as in the standard set up (Fast et al., 2006), with emissions specified on the fine grid in μg m^{-2} s^{-1}, except that the altitude of emission has been changed mimicking an injection of aerosols into the stratosphere (at a single model level at an altitude discussed below), and emission rates that are considerably larger than is typical for ob-
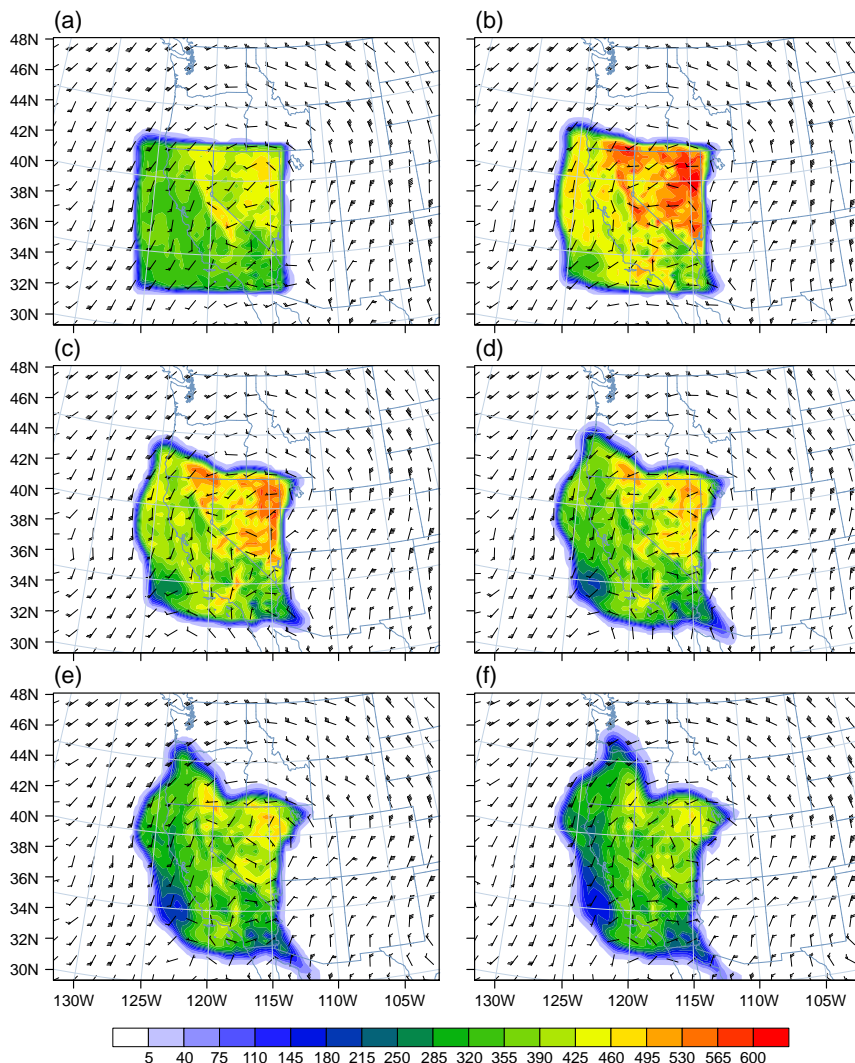
Fig. 4. Bin 2 sulfate aerosol concentrations [μg kg^{-1} of dry air] and wind barbs (kts) at the level of the injection in July 23rd at hours (a) 8:00 LT, (b) 10:00 LT, (c) 12:00 LT, (d) 14:00 LT, (e) 16:00 LT, and (f) 18:00 LT.

served surface sources. The evolution of the bin distribution and aerosol growth will be discussed in section 2.3.

Experiments are conducted over a range of different sulfate aerosol emissions rates (6, 10, 20, 30 and 60 μg m^{-2} s^{-1}) over a large-scale emissions area further discussed below. Results at example grid points, one in the Los Angeles region (34.05°N; 118.25°W) and another in the Central Valley region (Fresno, 36.75°N; 119.77°W), are seen as a function of the emission rate in Fig. 2. For the figures presented throughout, we have chosen the experiment with emissions rate of 30 μg m^{-2} s^{-1} as typifying the results. Given the magnitude of the surface temperature response (around 6°C at the time shown), this may be higher than would be required if such experiments were to be taken to a real-world application, but it produces a signal strong enough to be well above the level of numerical noise in the simulated response. Similar spatial patterns to those presented below are found in all experiments. The amplitude of the emissions will be discussed in more detail in section 2.2. For the time of the aerosol injection, we have chosen a two-hour period in the morning, from 6:00 LT to 8:00 LT local time, so we can see the effect of the aerosols on the full diurnal cycle. The experiment is repeated independently on each of two days of the heat wave (July 22nd and July 23rd, 2006), as discussed in section 2.3.

Figure 3 and Fig. 4 show the spatial patterns of sulfate concentrations in bin 2 evolving as a function of time on July 22nd and July 23rd from emissions in a simple square shape, referred to as the large-scale emissions experiment. Emissions over such a large-scale region would likely be imprac-
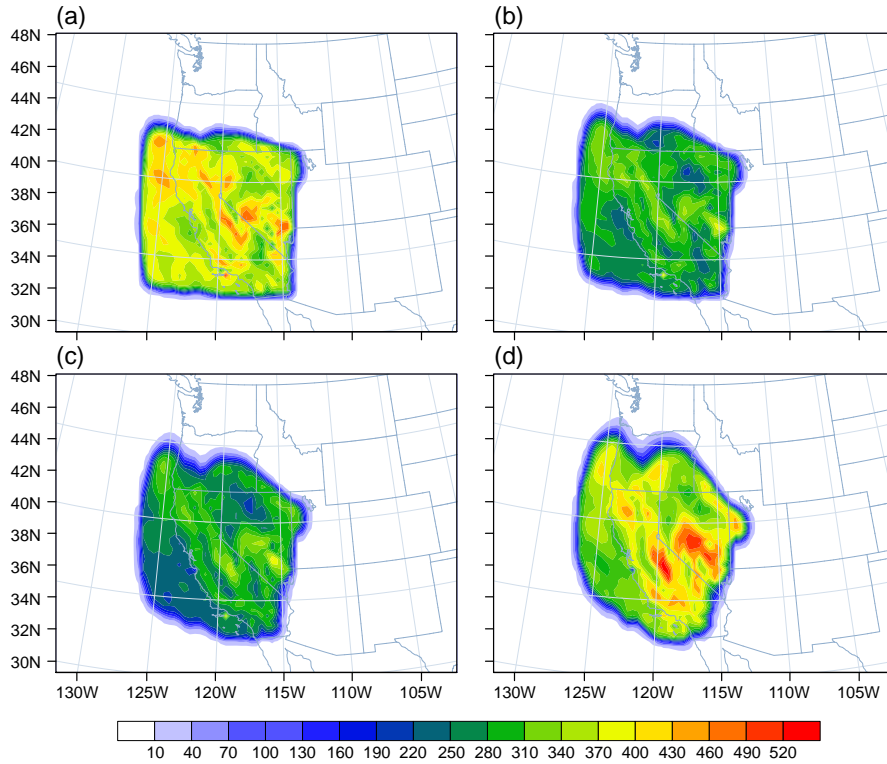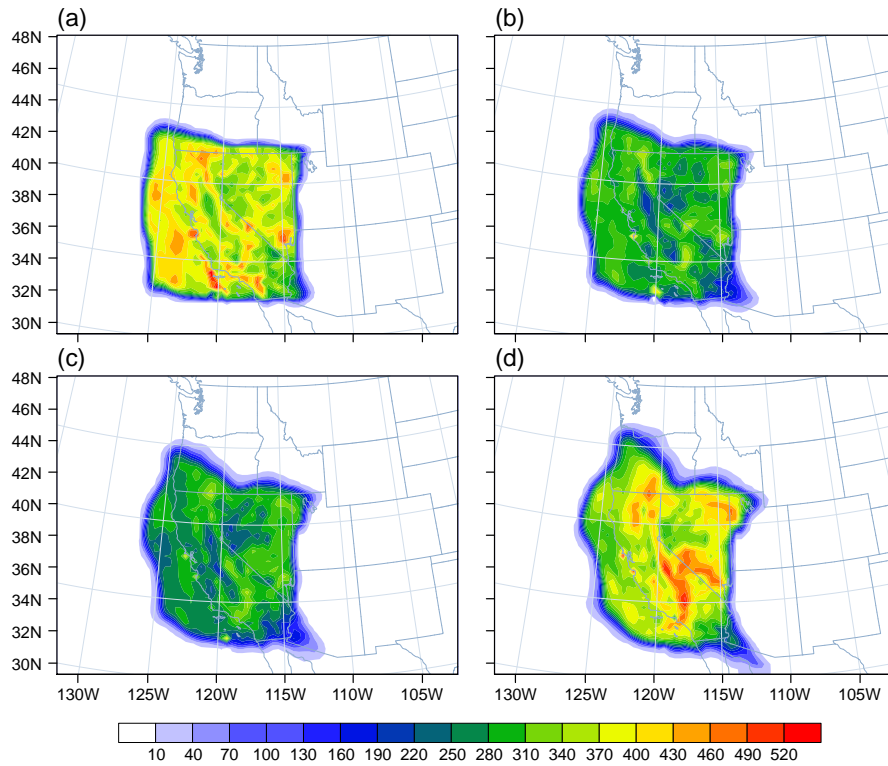
Fig. 5. Downward surface shortwave flux differences [W m^{-2}] between large-scale 30μg m^{-2} s^{-1} experiment and the control in July 22nd at hours (a) 10:00 LT, (b) 12:00 LT, (c) 14:00 LT, and (d) 16:00 LT.

tical for any real-world application but this experiment serves to illustrate regional differences in the temperature response under an area of relatively similar solar response. The key point from Fig. 3 is that advection does not rapidly carry the aerosol cloud outside of the domain, even for emissions in the lower stratosphere. Figure 3 also demonstrates the importance of vertical advection, not just horizontal, leading to the inhomogeneities in the concentrations inside of the emissions square. Furthermore, the level of aerosol injection has been chosen according to meteorology, an example of a strategy that can be advantageous to the regional application for each particular heat wave event. We chose the level of 12 kilometers as the level of aerosol injection, which has a relatively low wind speed, as estimated from the morning wind values over an important target region, Los Angeles. This helps reduce the rate at which the aerosol cloud is advected. This altitude is just above the cold-point tropopause—a level lower than would be typically chosen for a global application—and so also serves to illustrate a trade-off discussed in section 5.

2.2   Amplitude of the emissions.

Figure 2 shows each bin concentration together with surface temperature and surface shortwave radiation differences as a function of aerosol emissions for the two sample locations.

For both regions, there is a highly linear relation between emissions, sulfate concentrations in bin 2 and shortwave radiation differences, although the temperature response curve differs from one region to another. The temperature response curve has a linear relation with bin 2 concentrations and shortwave differences in the Central Valley area, reaching a reduction of about 11°C in the case of a 60 μg m^{-2} s^{-1} aerosol emission. In the Los Angeles area, the temperature response increases in the case of an aerosol emission higher than 6 μg m^{-2} s^{-1} and achieves a maximum of 8°C in the case of the highest aerosol emission rate. Each of the bin concentration curves behaves similarly in the two locations. The concentration curve of the first bin, which has the finest particles, increases and stabilizes after reaching 22 μg kg^{-1} of dry air at an aerosol emission of 6 μg m^{-2} s^{-1}. The concentration curve of bin 3 increases, since the aerosol emission is higher than 6 μg m^{-2} s^{-1}. The concentration of bin 4 is very low but shows a slight increase with aerosol emission increases. For the case of 30 μg m^{-2} s^{-1} aerosol emission, the shortwave reduction of about 200 W m^{-2} corresponds to approximately a 18% reduction in incoming surface shortwave relative to the control.

Fig. 6. Downward surface shortwave flux differences [W m^{-2}] between large-scale $30\mu g$ m^{-2} s^{-1} experiment and the control in July 23rd at hours (a) 10:00 LT, (b) 12:00 LT, (c) 14:00 LT, and (d) 16:00 LT.

2.3 Shortwave radiation and temperature for large-scale injection case

Figure 5 and Fig. 6 show the downward surface shortwave response at times corresponding to Fig. 3 and Fig. 4 respectively. In the middle of the day, the overall size of the impact is a decrease of about 350 W m^{-2}. Aerosols were injected during morning hours, between 6:00 LT and 8:00 LT. The selection of time for inserting aerosols depends on their not being carried out of the target region too quickly. Inserting them in the early-morning allows them more time to act before reaching the time of maximum temperature and aids examination of impact on the diurnal cycle.

The impact of these shortwave reductions by the aerosol cloud for surface air temperature may be seen in Fig. 7 and Fig. 8. For the chosen rate of emissions in this experiment, the impacts are substantial. Regional differences in the sensitivity of the response may be noted. One example is the greater Los Angeles region, which has less impact for a given level of sulfate aerosol concentrations than does the Central Valley. This appears to be consistent with the fact that the Los Angeles region tends to be strongly ventilated by wind flow from the ocean, while the Central Valley's maximum temperatures tend to be strongly affected by local balances involving radiative transfer and boundary layer turbulence.

Comparing the runs for July 22 and July 23rd indicates the modest effects of slightly different day to day flow patterns within the heat wave (July 23rd was slightly hotter than July 22nd). The results of sulfate concentration, downward shortwave flux differences, and surface air temperature are shown in Fig. 4, 8, and 6, respectively. The overall simulations for both days show a very similar pattern of surface shortwave and surface temperature differences. The simulations of both days show significantly higher temperature differences in the Central Valley, and the surface air temperature difference in the middle of the day reaches up to 7°C in that area. Thus to a first approximation, the shortwave and temperature differences may be taken as typical of what would result for other similar heat wave days in this region.

On both days, the surface air temperature changes are actually larger at the time of the morning temperature increase and the evening temperature decrease, which can be understood by examining the evolution through the course of the day.

As a prelude to this, Fig. 9 shows the sulfate concentration of each bin changing with time in the Los Angeles and the Central Valley areas. It shows rapid increase in the smallest-sized bin 1 during the two hours of the emission, and a sharp
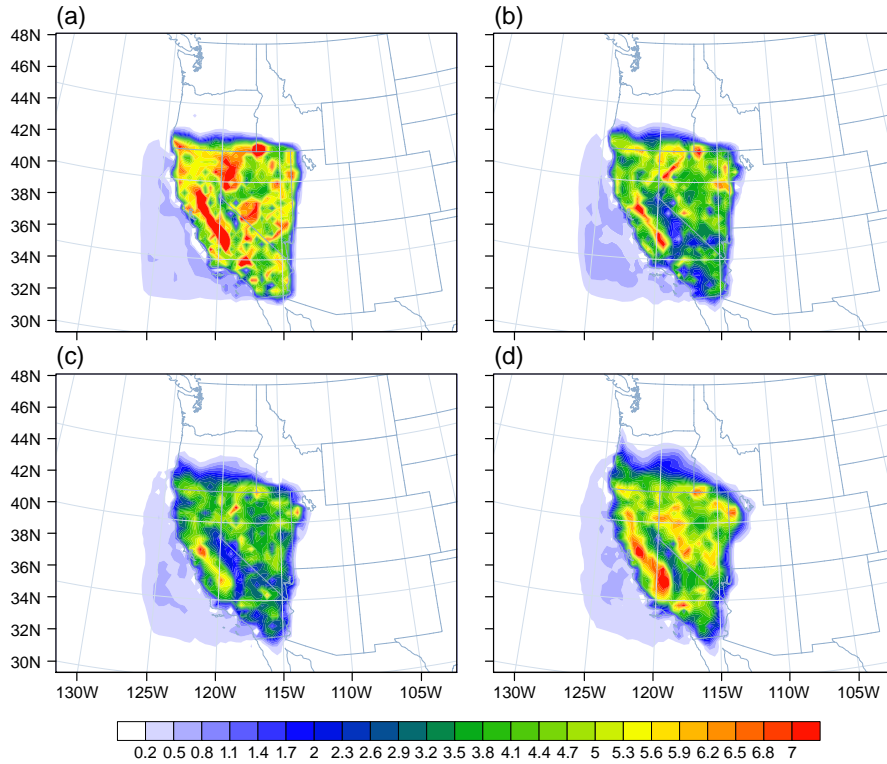
Fig. 7. Surface air temperature differences, [°C] between large-scale $30\mu g$ m^{-2} s^{-1} experiment and the control in July 22nd at hours (a) 10:00 LT, (b) 12:00 LT, (c) 14:00 LT, and (d) 16:00 LT.

decrease after the end of injection in the second hour. The bin 2 concentration increases for another two hours after the emission, associated with the conversion from bin 1 to 2. Bin 3 increases slowly with time and tending to stabilize several hours after the emission.

The downward shortwave radiation and surface temperature differences time-series are shown in Fig. 10 for the Los Angeles and the Central Valley areas for both July 22nd and July 23rd. The pattern of shortwave differences is similar for both days and for both areas. In each case, the shortwave reduction is slightly larger around 9:00 LT and 17:00 LT due to variation of total optical depth through the cloud with solar zenith angle. The temperature impact differs from the Los Angeles to the Central Valley areas. The Central Valley surface temperature impact has two clear peaks. One peak, of about 16° to 17°C, occurs in the morning at 9:00 LT, while the other peak, which reaches 19° to 21°C, occurs in the evening at 18:00 LT. The Los Angeles temperature impact has a peak of 7.5° to 9°C at 9:00 LT and another minor peak of about 5°C at 19:00 LT. In each case, the large peak in the difference corresponds to the time of rapid increase or decrease of total temperature at the beginning or end of the day, effectively shortening the hot part of the day. In the Central Valley, the local meteorological balances in the control run

yield the hottest part of the day in late afternoon, followed by a rapid drop in temperature, while in the experiment this is reduced by 7°C, followed by an earlier drop in temperature. In Los Angeles, the lag of the hot part of the day, and the subsequent temperature drop, are each smaller, and the reduction of temperature more constant in the experiment.

3   Smaller scale emission regions.

The large-scale idealized experiment serves to highlight regional differences in sensitivity and to provide a sense of the magnitude of temperature response for a given level of aerosol loading, but involves far larger emissions areas than would be under consideration for any practical implementation. We thus consider examples that move towards more localized emission regions. For efficiency of presentation, we show two localized regions in a single experiment. One over Southern California area and another one over southern part of San Joaquin Valley, which is part of the Central Valley. The initial area coverage of the two small scale emission regions is 69120 km^2 and 48384 km^2 respectively. The smaller is roughly 1/22 the size of the large-scale experiment emission area (the two together total about 1/9 of the large-scale experiment). These are each larger than would be used in
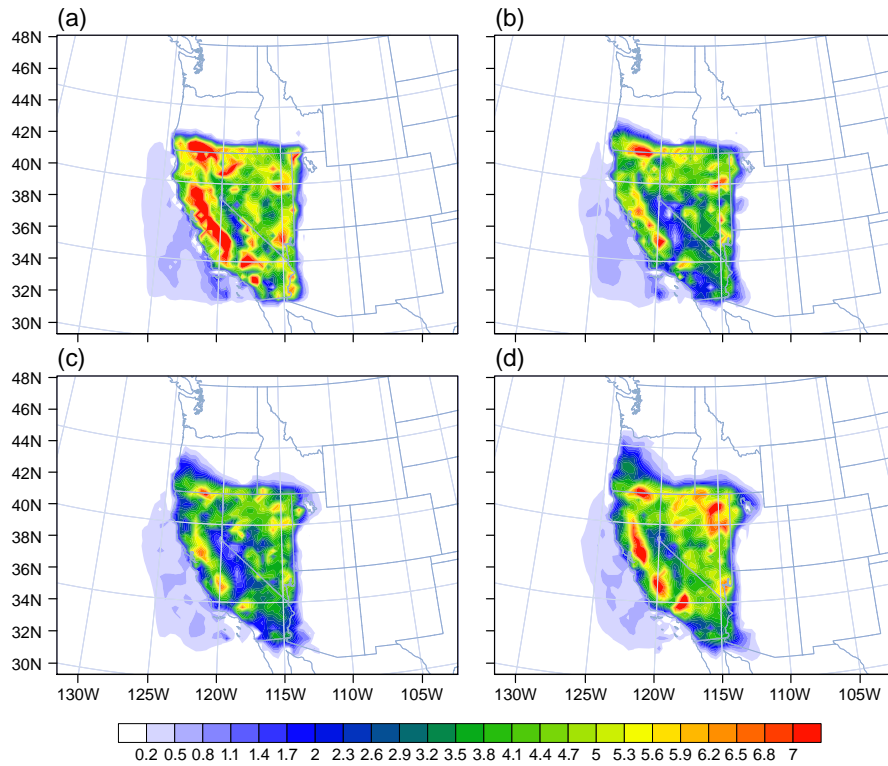
Fig. 8. Surface air temperature differences, [°C] between large-scale $30\mu g$ m^{-2} s^{-1} experiment and the control in July 23rd at hours (a) 10:00 LT, (b) 12:00 LT, (c) 14:00 LT, and (d) 16:00 LT.
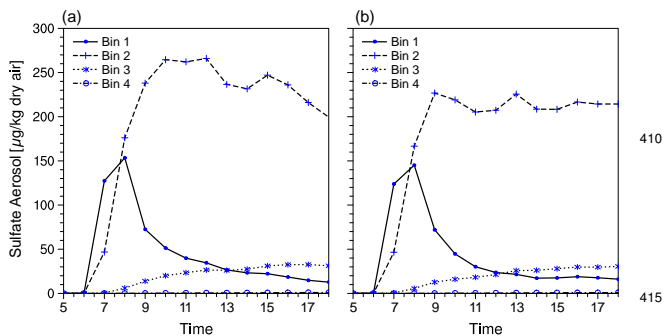

Fig. 9. Sulfate aerosol concentrations [μg kg^{-1} dry air] time-series (local time) at the level of the injection for July 22nd for a point locations (a) in Los Angeles and (b) in the Central Valley (Fresno). See Fig. 1 for point locations.

a practical application, but serve to illustrate the challenges that would arise at a regional scale. In particular, advective effects will become increasingly important to take into account with respect to specific target regions.

Here the examples provide shading, (i) to a region extending from the greater Los Angeles metropolitan area down to San Diego and a large region to the east, and (ii) to a region surrounding Fresno in the Central Valley and extending down to San Bernardino. It would be possible to tailor such regions more specifically to populated or agricultural areas, or to undertake continuous emissions upstream of the region. The latter would have the trade-off for a given amount of total emissions of spreading the emissions over a longer time interval. For simplicity, the example here is done with two hours of emissions in the morning, as in the large-scale experiment, with the emissions location and areal extent being estimated such that the cloud covers much of the target region for most of the day, even taking into account the advective movement. We use simple rectangular emission regions so it is easy to visualize the impact of advection, but of course this would be optimized in any practical application using weather forecasts for wind fields. The estimates here use 12 hour back trajectories from the HYbrid Single-Particle Lagrangian Integrated Trajectory (HYSPLIT) model (Draxler and Rolph, 2012).

Figure 11 and Fig. 12 show the surface shortwave and surface air temperature differences relative to the control resulting from these emissions patterns. At 10:00 LT, which is four hours after the injection, the cloud still resembles a slightly shifted and stretched version of the rectangular initial region.
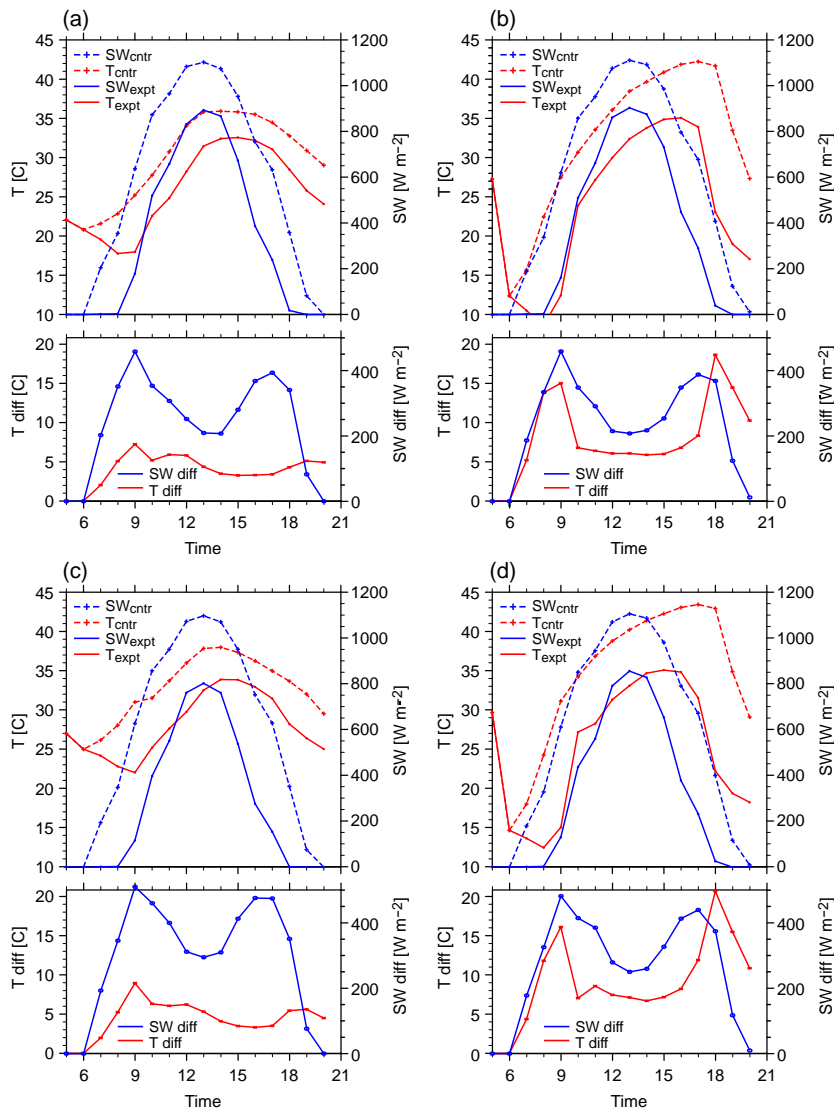
Fig. 10. Time-series (local time) of surface air temperature [°C] (red) and surface shortwave flux [W m^{-2}] (blue); the upper panel shows the control run and experimental surface air temperature and surface shortwave radiation flux, and the lower panel shows the differences between the control run and the experimental surface air temperature and surface shortwave radiation flux for (a) Los Angeles, July 22nd, (b) Central Valley (Fresno), July 22nd, (c) Los Angeles, July 23rd, (d) Central Valley (Fresno), July 23rd.

At 16:00 LT, the area of the aerosol cloud has altered substantially but in a manner that is largely predictable from the flow field. In this test, we choose an initial emission region such that the cloud would not drift over the ocean within 12 hours, although some part of the cloud covers unpopulated areas over the desert. From the evolution of the short wave pattern in Fig. 11, one can infer that coverage for an area comparable to Los Angeles could plausibly be achieved with overall emissions one quarter to one tenth the size, although this would require careful consideration of the flow pattern.

The amplitude of the shortwave difference and surface air temperature differences within each region are very similar to those in the large-scale area test shown in Fig. 5 and Fig. 7, but the values of shortwave and surface air temperature are slightly smaller due to the mixing of clean air from outside the cloud.

The smaller emission area that covers the Los Angeles Basin corresponds to approximately 15 Gg of sulfate aerosols or 3.75 Gg of sulfur [2 Tg SO$_2$=1 Tg S $\sim$ 4 Tg aerosol particles (Rasch et al., 2008a)] integrated over the region and over the two-hour emissions interval for a given day. Compared to the 10 Tg S annual injection under recent consider-
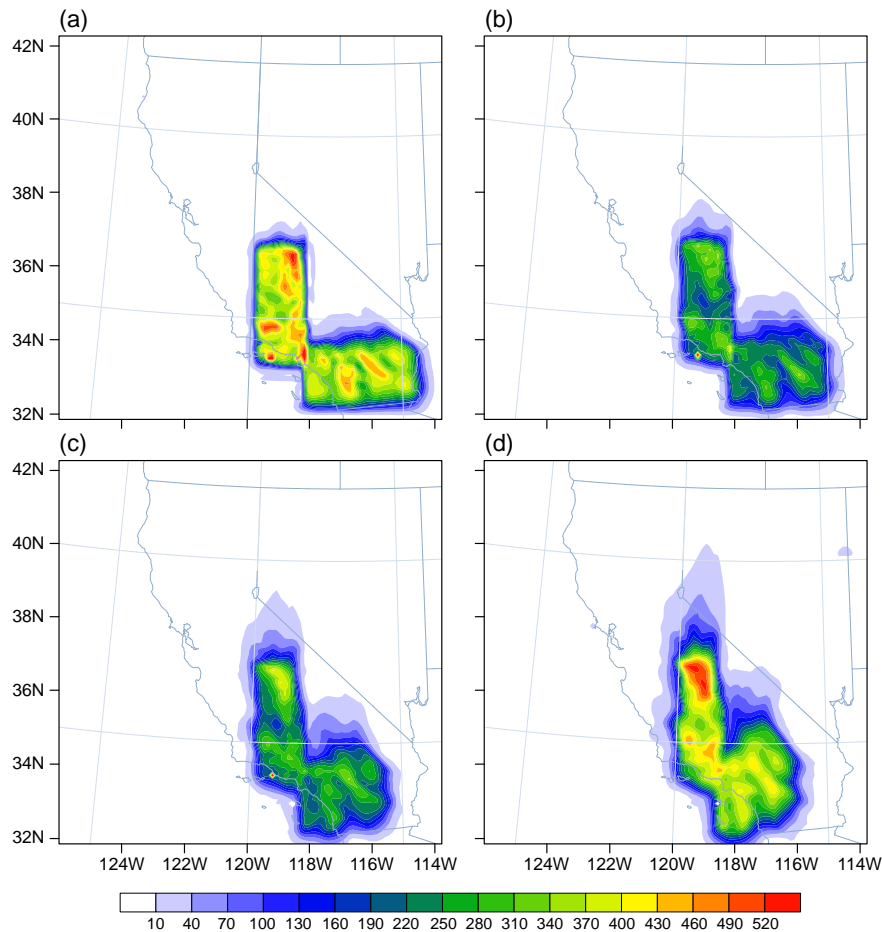
Fig. 11. Downward surface shortwave flux differences [W m^{-2}] in July 22nd at hours (a) 10:00 LT, (b) 12:00 LT, (c) 14:00 LT, and (d) 16:00 LT for the smaller-scale emissions experiments.

ation for global geoengineering considerations (Pierce et al., 2010; English et al., 2012), this is a small fraction: roughly 1/2700th the size in terms of sulfur equivalent. However, to provide a rough visualization of the mass of sulfate aerosols involved, this corresponds to a payload of about 120 C-5s, the largest US cargo jets, i.e., a very substantial mass. It must be underlined that this amount is for just one day, for one heat wave, and for the one specific region.

4 Testing via shortwave measurements.

In considering how one might test the effectiveness of such aerosol injections in a real-world experiment, the natural variability of temperature and the fact there is no control experiment must be taken into account. There would be no way of telling what temperature would have occurred in the absence of the aerosol release (Robock et al., 2010). However downward shortwave reductions, such as those shown in Fig. 5 and Fig. 11 and the corresponding upward reflected solar at the top of the atmosphere, could be directly measured. The aerosol cloud spatial pattern is initially highly identifiable and can be tracked through time. This process would be made easier in this application because heat waves tend to occur at times with small cloud cover. In conjunction with other measurements, the shortwave reduction could be attributed to the emissions with fairly high accuracy, and this can be used as the leading benchmark of the impact. To translate this to surface temperature reductions, one would then use data sets from comparable meteorological situations but with and without natural cloud cover to estimate the surface temperature reduction per decrease in surface shortwave flux.

5 Discussion and Conclusions.

This study critically examines the potential for an aerosol-injection geoengineering strategy to be applied at a regional scale to reduce the impacts of a heat wave. If geoengineering proposals come to be taken seriously at the global scale, there
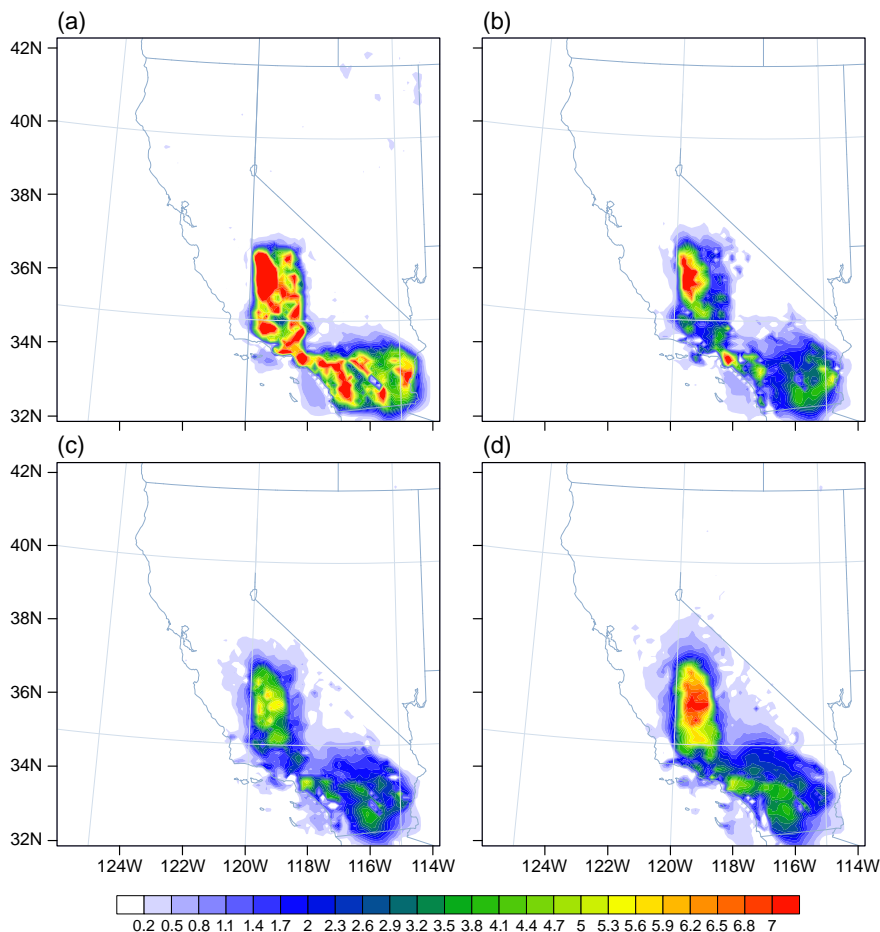
Fig. 12. Surface air temperature differences [°C] in July 22nd at hours (a) 10:00 LT, (b) 12:00 LT, (c) 14:00 LT, and (d) 16:00 LT for the smaller-scale emissions experiments.

may be increasing motivation to consider regional applica-505 tions, and so it is worth assessing in advance the size of the emissions required to have a regional impact, and the likely trade-offs and concerns. The sensitivity of surface tempera-490 ture and the advection effects at the altitude of injection will both depend on the meteorology of the particular heat wave.510 Thus a specific example is examined for the conditions of an observed heat wave with a regional scale model to provide a sense of how substantial these effects will be.

495 The results indicate that a sufficiently large injection of sulfate aerosols can indeed have a substantial impact on515 surface air temperature, although the temperature response varies among areas. For instance, temperature response in the Los Angeles area. 500 This is partially attributable to the topographical locations of the Central Valley and Los Angeles, as well as Los Angeles'520 close proximity to the Pacific Ocean, and was reproducible on both days of the 2006 heat wave. The temperature response during the hottest part of the day is a key factor in

reducing heat wave impacts, and is roughly 7°C in the Central Valley for the case of an injection of 30 μg m^{-2} s^{-1}. The temperature difference has a strong diurnal cycle, and is actually larger during the morning and late afternoon hours, due to the optical depth dependence on solar zenith angle. This has the effect of shortening the hot part of the day.

The temperature reduction scales approximately linearly with the magnitude of the aerosol injection, so the latter could be reduced to meet temperature targets. The flow field at the height of injection is a significant factor in the evolution of the aerosol cloud. Thus, the choice of the emission amplitude and height level would depend on the meteorology at the time of the heat wave. These appear to be within the realm that could be addressed by forecasting the flow, provided the emissions would be carried out over regions at least as large as a greater metropolitan area. The choice of the height of the emission based on flow field characteristics would yield a trade-off relative to choices that might be made for maximizing global scale impacts or minimizing down-

stream side effects. The case presented here uses a choice that might typify that of a decision-maker choosing the emission height based solely on local considerations of minimal flow for a specific city at a time just before the start of the emissions. The height used for illustration in this case is just above the cold-point tropopause, where the winds were relatively weak over Los Angeles for this case. This is at lower altitude than would be optimal from the perspective of global dispersion and of minimizing reentry into the troposphere in states downstream. This serves to illustrate that if such an approach were to be considered for actual application, there would need to be requirements established that those responsible for local emissions decisions consider the downstream effects.

For the emissions area covering most of Southern California considered in section 4, the sulfur equivalent of the aerosol injections on a given day is roughly 2700 times smaller than the 10 Tg annual emission of sulfur being considered for global applications. Even for smaller areas, this would represent a very substantial amount of aerosol to be lofted. Furthermore, this would have to be done repeatedly at each heat wave, and for each region. If one were in a situation of being committed to global geoengineering, the regional application might be worth consideration either as a means of testing the global application, or of timing the emissions to produce additional regional benefit in terms of temperature reduction during heat waves. Otherwise, regional planners might be well advised to consider other strategies involving regional adaptation of infrastructure to protect against heat wave impacts.

This is reinforced by the fact that, in addition to potential negative downstream impacts such as on precipitation, or ozone layer depletion (e.g., Robock, 2008), the regional application has an additional, very substantial potential downside. To protect a populated region from the effects of the heat wave using such a method, the emissions would have to be conducted over or just upstream from the populated area. This immediately raises the attendant concern for possible local negative effects or the public perception of these effects. Considerations for the local safety of the emission process would be much greater than those potentially arising from emissions over a remote, unpopulated region, as could be done for global geoengineering applications.

Thus while a regional scale application may have sufficient appeal to make it worth assessing in model simulations, the considerations noted here are consistent with recommendations from assessment of global scale applications (Robock et al., 2008; Heckendorn et al., 2009; English et al., 2012) that the downsides of geo-engineering with sulfate aerosols prevent considering them a good alternative to mitigation via reduction of fossil fuel emissions.

References

Bao, J. W., Michelson, S. A., Persson, P. O. G., Djalalova, I. V., and Wilczak, J. M.: Observed and WRF-simulated low-level winds in a high-Ozone episode during the Central California ozone study, J. Appl. Meteorol. Clim., 47, 2372–2394, 2008.

Barnard, J. C., Fast, J. D., Paredes-Miranda, G. , Arnott, W. P., and Laskin, A.: Technical note: evaluation of the WRF-Chem aerosol chemical to aerosol optical properties module using data from the MILAGRO campaign, Atmos. Chem. Phys., 10, 7325–7340, 2010.

Brovkin, V., Petoukhov, V., Claussen, M., Bauer, E., Archer, D. , and Jaeger, C.: Geoengineering climate by stratospheric sulfur injections: Earth system vulnerability to technological failure, Climatic Change, 92, 243–259, 2009.

Budyko, M. I.: Climate and Life, Academic Press, New York, USA, 508 pp.,1974.

Chan, A. K., Hyde, R. A., Myhrvold, N. P., Tegreene, C. T., and Wood, L. L.: High Altitude atmospheric injection system and method, US Patent Application Publication: US 2010/0071771, Publication Date: March 25, 2010.

Chapman, E. G., Gustafson Jr., W. I., Easter, R. C., Barnard, J. C., Ghan, S. J., Pekour, M. S., and Fast, J. D.: Coupling aerosol-cloud-radiative processes in the WRF-Chem model: Investigating the radiative impact of elevated point sources, Atmos. Chem. Phys, 3, 945–964, 2009.

Chen, D., Li, Q., Fovell, R. G., Li, Z., Stutz, J., Mao, Y., Zhang, L., Pikelnaya, O., Tsai, J. Y., Haman, C., Lefer, B., de Gouw, J., Holloway, J., Murakami, J., and Ryerson, T.: WRF-Chem simulation of meteorology and CO in the Los Angeles basin during CalNex-2010, in preparation.

Chen, F. and Dudhia, J.: Coupling an advanced land-surface (hydrology model with the Penn State (NCAR MM5 modeling system. Part I: Model description and implementation, Mon. Weather Rev., 129, 569585, doi:10.1175/1520-0493, 2001.

Crutzen, P. J.: Albedo enhancement by stratospheric sulfur injections: A contribution to resolve a policy dilemma?, Climatic Change, 77, 211–220, 2006.

Draxler, R. R. and Rolph, G. D.: HYSPLIT (HYbrid Single-Particle Lagrangian Integrated Trajectory) Model access via NOAA ARL READY Website (http://ready.arl.noaa.gov/HYSPLIT.php), NOAA Air Resources Laboratory, Silver Spring, MD, 2012.

Dudhia, J.: Numerical study of convection observed during the winter monsoon experiment using a mesoscale two-dimensional model, J. Atmos. Sci., 46, 3077-3107, 1989.

English, J. M., Toon, O. B., and Mills, M. J.: Microphysical simulations of sulfur burdens from stratospheric sulfur geoengineering, Atmos. Chem. Phys., 12, 2517-2558, doi:10.5194/acpd-12-2517-2012, 2012.

Fast, J. D., Gustafson Jr., W. I., Easter, R. C., Zaveri, R. A., Barnard, J. C., Chapman, E. G., Grell, G. A., and Peckham, S. E.: Evolution of ozone, particulates, and aerosol direct radiative forcing in the vicinity of Houston using a fully coupled meteorology-chemistry-aerosol model, J. Geophys. Res., 111, D21305, 2006.

Gershunov, A., Cayan, D. R., and Iacobellis, S. F.: The great 2006 heat wave over California and Nevada: Signal of an increasing trend, J. Climate, 22, 6181–6203, 2005.

Ghan, S., Laulainen, N., Easter, R., Wagener, R., Nemesure, S., Chapman, Y., Zhang, E., and Leung, R.: Evaluation of aerosol direct radiative forcing in MIRAGE, J. Geophys. Res., 106, 5295–5316, 2001.

Grell, G. A. and Devenyi, D.: A generalized approach to parameterizing convection combining ensemble and data assimilation techniques, Geophys. Res. Lett., 29, 1693, doi:10.1029/2002GL015311, 2002.

Grell, G. A., Peckham, S. E., Schmitz, R., McKeen, S. A., Frost, G., Skamarock, W. C., and Eder, B.: Fully coupled "online" chemistry within the WRF model, Atmos. Environ., 37, 6957 – 6975, 2009.

Grell, G. A.: Coupled weather chemistry modeling, in: Large-scale disasters: prediction, control, mitigation, Mohamed Gad-el-Hak, Cambridge University Press, 302–317, 2008.

Grell, G. A., Fast, J. D., Gustafson, Jr., W. I., Peckham, S. E., McKeen, S. A., Salzmann, M., and Freitas, S.: On-line chemistry within WRF: description and evaluation of a State-of-the-Art multiscale air quality and weather prediction model, in: Integrated systems of meso-meteorological and chemical transport models, Springer, Baklanov, A., Mahura, A., and Sokhi, R., 41–54, 2011.

Heckendorn, P., Weisenstein, D., Fueglistaler, S., Luo, B. P., Rozanov, E., Schraner, M., Thomason, L. W., and Peter, T.: The impact of geoengineering aerosols on stratospheric temperature and ozone, Environ. Res. Lett., 4, 045108, 2009.

Hong, S.-Y., Dudhia, J., and Chen, S.-H.: A revised approach to ice microphysical processes for the bulk parameterization of clouds and precipitation, Mon. Weather Rev., 132, 103–120, 2004.

Jones, A., Haywood, J., Boucher, O., Kravitz, B., and Robock, A.: Geoengineering by stratospheric SO_2 injection: results from the Met Office HadGEM2 climate model and comparison with the Goddard Institute for Space Studies ModelE, Atmos. Chem. Phys., 10, 7421–7434, 2010.

Intergovernmental Panel on Climate Change: Contribution of Working Group I to the Fourth Assessment Report of the Intergovernmental Panel on Climate Change, Climate Change 2007: The Physical Science Basis, Solomon, S., Qin, D., Manning, M., Chen, Z., Marquis, M., Averyt, K. B.,Tignor, M., and Miller, H. L., Cambridge University Press, Cambridge, UK, 2007.

Klemp, J. B., Skamarock, W.C., and Dudhia, J.: Conservative split-explicit time integration methods for the compressible nonhydrostatic equations, Mon. Weather Rev., 135, 2897– 2913, 2007.

Kravitz, B., Robock, A., Oman, L., Stenchikov, G., and Marquardt, A.B.: Sulfuric acid deposition from stratospheric geoengineering with sulfate aerosols, J. Geophys. Res., 114, D14109, 2009.

Kravitz, B., Robock, A., Boucher, O., Schmidt, H., Taylor, K. E., Stenchikov, G., and Schulz, M.: The Geoengineering Model Intercomparison Project (GeoMIP), Atmos. Sci. Lett., 12, 162–167, 2011.

Lu, W., Zhong, S., Charney, J. J., Bian, X., and Liu, S.: WRF simulation over complex terrain during a southern California wildfire event, J. Geophys. Res., 117, D05125, 2012.

Matthews, H. D. and Caldeira, K.: Transient climatecarbon simulations of planetary geoengineering, P. Natl. Acad. Sci. USA, 104, 9949–9954, 2007.

Mesinger, F., Dimego, G., Kalnay, E., Mitchell, K., Shafran, P. C., Ebisuzaki, W., Jovi, D., Woollen, J., Rogers, E., Berbery, E. H., Ek, M. B., Fan, Y., Grumbine, R., Higgins, W., Li, H., Lin, Y., Manikin, G., Parrish, D., and Shi, W. : North American Regional Reanalysis, B. Am. Meteorol. Soc., 87, 343360, doi: http://dx.doi.org/10.1175/BAMS-87-3-343, 2006.

Niemeier, U., Schmidt, H., and Timmreck, C.: The dependency of geoengineered sulfate aerosol on the emission strategy, Atmos. Sci. Lett., 12, 189–194, 2011.

Ostro, B. D., Roth, L. A., Green, R. S., and Basu, R.: Estimating the mortality effect of the July 2006 California heat wave, Environ. Res., 109, 614–619, 2009.

Pierce, J. R., Weisenstein, D. K., Heckendorn, P., Peter, T., and Keith, D. W.: Efficient formation of stratospheric aerosol for climate engineering by emission of condensible vapor from aircraft, Geophys. Res. Lett., 37, L18805, doi:10.1029/2010GL043975, 2010.

Rasch, P. J., Crutzen, P. J., and Coleman, D. B.: Exploring the geoengineering of climate using stratospheric sulfate aerosols: The role of particle size, Geophys. Res. Lett., 35, L02809, 2008.

Rasch, P. J., Tilmes, S., Turco, R. P., Robock, A., Oman, L., Chen, C., Stenchikov, G. L., and Garcia, R. R.: An overview of geoengineering of climate using stratospheric sulphate aerosols, Philos. T. Roy. Soc. A, 366, 4007–4037, 2008a.

Robock, A.: The climatic aftermath, Science, 295, 1242–1244, 2002.

Robock, A.: 20 reasons why geoengineering may be a bad idea, B. Am. Meteorol. Soc., 64, 14–18, 2008.

Robock, A., Oman, L., and Stenchikov, G. L.: Regional climate responses to geoengineering with tropical and Arctic SO_2 injections, J. Geophys. Res., 113, D16101, doi:10.1029/2008JD010050, 2008.

Robock, A., Marquardt, A., Kravitz, B., and Stenchikov, G.: Benefits, risks, and costs of stratospheric geoengineering, Geophys. Res. Lett., 36, L19703, 2009.

Robock, A., Bunzl, M., Kravitz, B., and Stenchikov, G. L.: A Test for geoengineering?, Science, 327, 530–531, 2010.

Tilmes, S., Mller, R., and Salawitch, R.: The sensitivity of polar ozone depletion to proposed geoengineering schemes, Science, 320, 1201–1204, 2008.

Trenberth, K. E., and Dai, A.: Effects of Mount Pinatubo volcanic eruption on the hydrological cycle as an analog of geoengineering, Geophys. Res. Lett., 34, L15702, doi:10.1029/2007GL030524, 2007.

Tzivion, S., Feingold, G., and Levin, Z.: The evolution of raindrop spectra. Part II: collisional collection/breakup and evaporation in a rainshaft, J. Atmos. Sci., 46, 3312-3327, 1989.

Volodin, E. M., Kostrykin, S. V., and Ryaboshapko, A. G.: Climate response to aerosol injection at different stratospheric locations, Atmos. Sci. Lett., 12, 381–385, 2011.

Wigley, T. M. L.: A Combined mitigation/geoengineering approach to climate stabilization, Science, 314, 452-454, 2006.

Zaveri, R. A., Easter, R. C., Fast, J. D., and Peters, L. K.: Model for Simulating Aerosol Interactions and Chemistry (MOSAIC), J. Geophys. Res., 113, D13204, 2008.